Journal of Power Sources 624 (2024) 235575

Contents lists available at ScienceDirect

Journal of Power Sources

journal homepage: www.elsevier.com/locate/jpowsour

Amide-based Al electrolytes and their application in Al metal anode-organic batteries

Matea Raić [a,b,1], Olivera Lužanin [b,c,1], Ivan Jerman [b], Robert Dominko [b,c,d], Jan Bitenc [b,c,*]

[a] Ruđer Bošković Institute, Bijenička C. 54, 10000, Zagreb, Croatia
[b] National Institute of Chemistry, Hajdrihova 19, 1001, Ljubljana, Slovenia
[c] Faculty of Chemistry and Chemical Technology, University of Ljubljana, Vecna Pot 113, 1000, Ljubljana, Slovenia
[d] Alistore-European Research Institute, CNRS FR 3104, Hub de L'Energie, Rue Baudelocque, 80039, Amiens, France

HIGHLIGHTS

- Different alkylamide-based Al electrolytes are investigated as cost-effective alternatives.
- Amide-based Al electrolytes enable high Al metal plating/stripping efficiency.
- Good capacity utilization and improved compatibility with organic cathodes.
- Increased length of amide alkyl chain leads to improved electrochemical performance.
- Identified a drawback of limited oxidative stability amide-based electrolytes.

ARTICLE INFO

Keywords:
Al electrolytes
Amides
Deep eutectic solvents
Al metal anode
Organic cathode
Electrochemical mechanism

ABSTRACT

Aluminum rechargeable batteries are seen as a next-generation battery technology based on abundant materials. However, the current standard Al electrolytes are based on expensive ionic liquids. In this paper, the potential use of three $AlCl_3$/amide-based electrolytes is investigated as a low-cost alternative from the perspective of Al metal anode and organic cathode compatibility. Our investigation shows the promising electrochemical performance of amide electrolytes and specific differences between the electrolytes depending on amide alkyl chain length. In particular, amides with longer alkyl chains show better plating/stripping efficiency and lower overpotential compared to the shorter acetamide one. Similarly, organic cathode capacity retention is the best for the electrolyte with the longest alkyl chain. However, the cathode capacity retention is subpar to the standard ionic liquid-based Al electrolyte although it undergoes the same electrochemical mechanism of carbonyl bond reduction. Interestingly, there is no deterioration of the anthraquinone redox peak through the appearance of a side peak at a lower potential in amide-based electrolytes, which is observed in standard electrolyte based on ionic liquid. Amide-based electrolyte display promise for practical applicability, however, the low oxidation stability of amide-based electrolytes is identified as one of their key limitation and should be addressed in future work.

1. Introduction

Li-ion batteries (LIBs) are currently the dominant battery technology, as well as a key technology for portable electronics, electromobility applications and stationary energy storage. However, there is an intense exploration of new materials and battery concepts in the field. The main goal is the development of alternative technologies that could potentially complement or replace LIBs in the future. The scarcity of certain natural resources like Li, Co and Ni coupled with increasing demand could make current LIBs unsustainable in the long run. EU has already identified most of the raw materials used in LIBs as critical raw materials (CRMs) either due to limited material resources or potential supply risks [1]. Furthermore, considerations regarding the environmental impact of mining and disposal of these materials are inciting

* Corresponding author. National Institute of Chemistry, Hajdrihova 19, 1001, Ljubljana, Slovenia.
E-mail address: jan.bitenc@ki.si (J. Bitenc).
[1] These authors contributed equally to this work.

https://doi.org/10.1016/j.jpowsour.2024.235575
Received 20 May 2024; Received in revised form 7 August 2024; Accepted 2 October 2024
Available online 17 October 2024

interest in alternative battery technologies [2]. Al batteries represent a highly prospective battery technology due to the promising properties of Al metal. Aluminum is the 3rd most abundant element in the Earth's crust, lightweight and relatively low cost. Al metal anode has high gravimetric (2981 mAh g^{-1}) and the highest volumetric capacity (8048 mAh cm^{-3}) among all elements. Al metal volumetric capacity is four times higher than Li metal anode and an order of magnitude higher than graphite anode (837 mAh cm^{-3}) used in contemporary LIBs [3,4]. The stability of Al metal upon air and water exposure simplifies handling and manufacturing, as well as safety, compared to highly reactive alkali metals like Li and Na [5–7].

The development of Al batteries moved into the spotlight in 2015 when Dai et al. reported a rechargeable battery with high-rate capability and long-cycle life containing an aluminum metal anode and graphitic foam cathode in a eutectic mixture of $AlCl_3$/1-ethyl-3-methyl-imidazolium chloride ionic liquid [8]. However, in this Al-graphite battery cell, instead of Al^{3+} cations being inserted into graphite, $AlCl_4^-$ anions were utilized. Insertion of the $AlCl_4^-$ anion meant consumption of $AlCl_3$-based electrolyte as anolyte instead of Al metal and severely reduced the maximum anode/anolyte capacity to only 49 mAh g^{-1}, almost two orders of magnitude lower than Al metal anode. To fully utilize the high capacity of the Al metal anode and achieve Al^{3+} utilization, several different materials were investigated, such as transition metal oxides, sulfur, sulfides, selenides and Prussian blue analogues [9]. Unfortunately, the majority of the studies report limited reversibility accompanied by rapid capacity fade since the insertion of the Al^{3+} cation is challenging due to the high charge density and strong interaction with the inorganic host. Recently, organic cathodes such as anthraquinone, polythiophene and phenanthrenequinone demonstrated an opportunity to circumvent the poor reversibility of inorganic hosts and store positively charged chloroaluminate species [10–12]. However, the utilization of chloroaluminate species, $AlCl_x^{(3-x)+}$ in organic cathodes is still affecting the anode capacity due to the utilization of $AlCl_3$-based electrolyte in the formation of active species. Nevertheless, anode/anolyte capacity is significantly increased due to the decreased amount of $AlCl_3$ needed to form positively charged chloroaluminate species $AlCl_x^{(3-x)+}$ (x being 1 or 2) instead of $AlCl_4^-$ [12].

The early development of Al electrolytes was primarily focused on Al metal electroplating, which involved the use of organic chloride salts and ionic liquids (IL) to effectively reduce the melting temperature of ionic melts used for electroplating [13–15]. Currently, many research efforts are focused on the development of alternative electrolytes based on deep eutectic solvents (DES), which would have similar properties as ILs but would be more cost-effective and eco-friendly [16–18]. DESs are created by combining a strong Lewis acidic metal halide with a Lewis base ligand. The formation of DES involving aluminum chloride ($AlCl_3$) and amides can indeed result in various Al species such as $AlCl_4^-$, $Al_2Cl_7^-$ and $[AlCl_2(amide)_n]^+$, depending on the molar ratio of $AlCl_3$ to the amide [19]. Electroplating of Al metal occurs only in the acidic melt in the presence of $Al_2Cl_7^-$ through the following reactions [7,20]:

$$4Al_2Cl_7^- + 3e^- \rightarrow Al + 7AlCl_4^- \quad (1)$$

$$AlCl_2(amide)_n^+ + 2Al_2Cl_7^- + 3e^- \rightarrow Al + 4AlCl_4^- + n(amide) \quad (2)$$

Acetamide is a Lewis base in alternative DES electrolytes. Recent studies have reported that an acetamide/$AlCl_3$ electrolyte can electrodeposit aluminum reversibly at room temperature [21–23]. Acetamide coordinates with $AlCl_2^+$ to form $[AlCl_2(acetamide)_2]^+$ [9]. Furthermore, not only acetamide (AAm) but also other amides (propionamide-PAm, butyramide-BAm) exhibit good ionic conductivity suitable for electrolyte applications [24]. The stability of amides in the presence of air and moisture is an important consideration for the practical manufacturing of the cell, as well as battery safety and storage. Given the low cost of amides (Table S1), which are several times cheaper than commonly used chloride-based ionic liquid, Al batteries using amides could offer considerable economic benefits, especially given the relatively large share of Al electrolyte in the cost of the Al battery system [22], which was in recent techno-economic analysis estimated at 28 % [25].

One of the critical aspects that determine the lifetime and performance of rechargeable batteries employing metal anodes is the efficiency of metal plating and stripping processes. In practical applications, very high cycling efficiencies, much higher than 99 %, are needed. Targeting efficiencies <99.9 % for long-term applications represents a significant milestone in the advancement of the technology. Even with a very high efficiency of 99.9 %, there can still be a significant capacity loss over several hundreds of cycles and a significant need to oversize electrode capacity for long-cycle life cells [26]. Achieving such high efficiencies of Al metal anodes could require a combination of material selection, such as the current collector selection, anode morphology and surface pretreatment, electrolyte optimization, as well as battery design.

In the present work, we prepared $AlCl_3$-amide-based electrolytes using three different amides: AAm, PAm and BAm and tested their electrochemical performance through Al metal plating/stripping in the conventional cycling protocol as well as macro-cycling procedure [27]. In the second part, we benchmarked the electrochemical performance of an organic cathode with all three amide analogues: AA, PA and BA versus standard ionic liquid-based electrolyte. Overall, longer alkyl chains of amides contribute to improved Al plating/stripping efficiency, lower overpotential and improved organic cathode capacity retention, exposing interesting directions for future research.

2. Experimental

Electrolytes were prepared in an Ar-filled glovebox (<1 ppm O_2, <1 ppm H_2O). The anhydrous $AlCl_3$ (Sigma Aldrich, 99 %) was used as received, while commercial amides (Sigma Aldrich, AAm ≥99.0 %, PAm 97 %, BAm ≥98.0 %) were dried under vacuum. $AlCl_3$-amide electrolytes were prepared by slowly adding amides to $AlCl_3$ powder due to a highly exothermic reaction. After mixing, a light-yellow liquid was formed. Subsequently, Al metal foil (Chempur) was added to the electrolytes and mixed for 4 h. The molar ratio between $AlCl_3$ and amides was 1.5:1 for all three amides.

Poly(anthraquinone sulfide) (PAQS) was synthesized as a nanocomposite with multi-walled carbon nanotubes (MWCNTs), according to the previously published procedure [28]. Details of the polymer synthesis and characterization are available in the Supporting Information (Fig. S1). Electrodes were prepared by mixing PAQS, Printex XE2 carbon black (Degussa), and PTFE binder (Sigma Aldrich, 60 % water dispersion) in a weight ratio of 6:3:1 in a dispersion of isopropanol. The mixture was then subjected to a planetary ball milling (Retsch PM100, 300 rpm for 30 min). A gum-like composite was rolled into a thin film between a glass plate and parchment paper. Self-standing 12 mm discs were then cut and dried at 50 °C overnight prior to cell assembly.

2.1. Electrochemical characterization

Cells were assembled in inside glovebox using two glass-fiber separators (GF/A Whatman) wetted with 80 μL of electrolyte. The electrochemical testing was carried out in two-electrode pouch cells using VMP3 and MPG2 potentiostats (Bio-Logic). Al plating/stripping tests were performed using two different electrochemical protocols, both utilizing Mo (0.025 mm, Alfa Aesar) working electrode (WE) and Al metal counter electrode (CE). In the first, more traditional protocol, Al metal was plated for 60 min at 0.1 mA cm^{-2} current density, followed by Al stripping until a cut-off voltage of 1.5 V for 100 cycles. The second protocol employed macro-reversible cycling, which started with Al plating for 5 h at 0.1 mA cm^{-2} current density, in which a larger amount of Al metal was plated. The next step was stripping of Al metal with the same current density for 1 h, (presumed stripping of only 20 % of deposited Al metal) [27]. This was followed by repeated Al plating/stripping for 1 h at 0.1 mA cm^{-2} for 100 cycles. Finally, the remaining Al metal was stripped until a cut-off voltage of 1.5 V was

reached. The electrochemical stability window was assessed using linear sweep voltammetry (LSV) using a Mo working electrode with a sweep rate of 0.1 mV s^{-1}.

The performance of electrolytes was tested in a full Al metal-organic cathode cell and benchmarked versus standard EMIMCl (Sigma Aldrich, 98 %): $AlCl_3$ = 1:1.5 electrolyte (EA). In all our tests we used PAQS/CNT as cathode active material. Cells were cycled in the voltage window from 0.4 to 1.8 V with a current density of 50 mA g^{-1} calculated on the amount of the active material. The active material loading of organic electrodes was between 1.5 and 2.5 mg cm^{-2}.

Organic electrodes for ex situ measurements were cycled using the same cell setup and conditions as in normal cycling. Based on long-term cycling performance, cathodes were harvested from pouch cells in the 2nd charge/discharge (AA, PA and EA), while BA was cycled for 10 cycles. Afterwards, the cells were disassembled inside the glovebox and electrodes were washed using dry THF three times. Infrared measurements were performed inside the glovebox using Bruker Alpha II, in the range from 4000 to 600 cm^{-1} with a resolution of 4 cm^{-1}.

3. Results and discussion

A molar ratio of $AlCl_3$:amide in the electrolyte to 1.5 was selected based on the literature report as the most optimal [29]. After preparing electrolytes, Raman spectroscopy was used to investigate Al species. Raman spectra in Fig. 1b identify two specific chloroaluminate complexes, $AlCl_4^-$ and $Al_2Cl_7^-$, with corresponding Raman shifts at 347 and 310 cm^{-1} in all three electrolytes [24]. The integral area percentage of intensity $Al_2Cl_7^-$ to $AlCl_4^-$ is represented with an I_{310}/I_{347} ratio in Table S2. Although the exact ratios between the peaks differ from the literature [29], a similar trend is observed with an increasing ratio of I_{310}/I_{347} corresponding with the increasing length of the alkyl chain of the amide, with the lowest ratio observed for AA and the highest for BA electrolyte.

Afterwards, the electrochemical stability window of the electrolytes was assessed with LSV using Mo as the working electrode (Fig. 1c). All electrolytes exhibit good stability beyond 1.8 V. Around 1.9 V, we already observe some initial oxidation current for PA and BA electrolytes, while in AA oxidation occurs at a slightly higher voltage. Around 0.5 V above initial oxidation currents, the oxidation process intensifies for all three electrolytes. LSV measurements confirm that all three electrolytes should be stable in the electrochemical window up to 1.8 V.

Al metal plating/stripping was assessed using the same electrochemical setup with a Mo metal working electrode (Fig. 2). The reversibility is assessed through Coulombic efficiency (CE) during the repeated plating/stripping process. The initial CE for all three electrolytes was close to 96 %, most likely caused by conditioning of electrolyte and removal of electrolyte impurities. We observed a gradual increase in the CE values and a drop of overpotential for all three electrolytes (Fig. S2). The CE for the PA and BA electrolytes was stabilized after 25 consecutive plating/stripping steps, while AA electrolyte displays less stable cycling and significantly lower plating/stripping efficiency. The average efficiencies were 97.6 %, 98.9 % and 98.6 % for AA, PA and BA, respectively (Table 1). Interestingly, a similar trend was observed when comparing cells' overpotential, where AA exhibits a higher overpotential, around 120 mV, whereas PA and BA exhibit similar overpotential, around 90 mV (values read out towards the end of the galvanostatic cycle).

Macro-reversibility test was applied to probe the Al plating/stripping under more realistic conditions. In this test, a larger amount of Al metal is plated on the WE at the start of the cycling process and Al metal is only partially stripped/plated from WE in each cycle. In our procedure, 0.5 mAh cm^{-2} of Al metal was plated on the WE in the first cycle (Fig. S3). In the following cycles, only 20 % (0.1 mAh cm^{-2}) of the initially plated Al metal is cycled in each cycle similar as in conventional cycling procedure, until in the final cycle the Al metal is completely stripped away until the cut-off voltage of 1.5 V. This procedure mimics cycling in a symmetrical cell while at the same time providing Al plating/stripping Coulombic efficiency. It has the downside of providing only the average Coulombic efficiency of the whole cycling process and no information about the changes in Al plating/stripping efficiency during cycling. A comparison of the average Coulombic efficiency for conventional and macro-reversible cycling shown in Table 1 displays specific differences in electrochemical performance between amides, a decrease in the efficiency in the case of AA, and higher efficiency for PA and BA electrolytes. Prolonged exposure of Al metal deposits throughout the macrocycling procedure increases sensitivity to degradation processes on Al metal deposits. A drop in the Coulombic efficiency of AA electrolyte could be caused by either passivation or poor adhesion of Al deposits. Overall better performance of PA and BA electrolytes could be assigned to a more stable metal/electrolyte interface in these electrolytes or more facile dissociation of $AlCl_2(amide)_n^+$ complexes in case of longer chain amides. Al plating/stripping was also electrochemically evaluated using

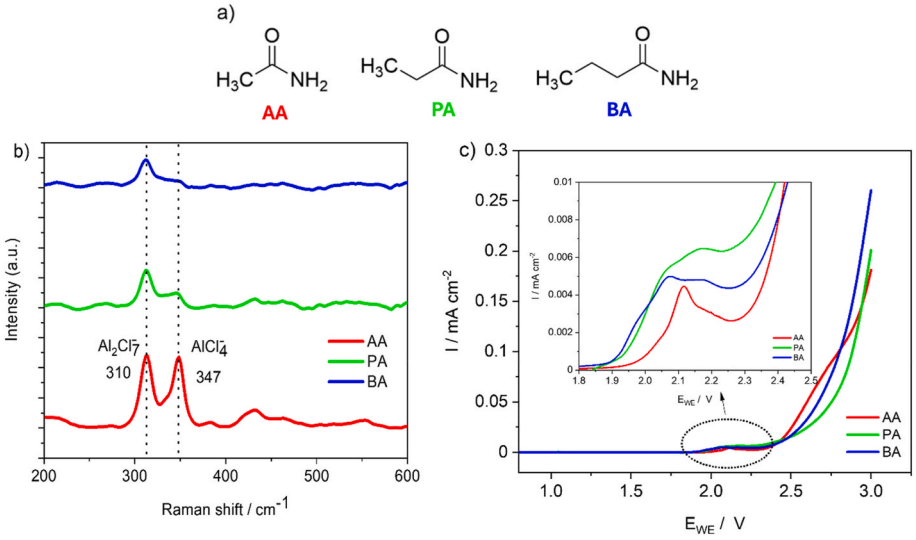

Fig. 1. a) Chemical structures of amides used for preparation of Al electrolytes. b) Raman spectra of $AlCl_3$-amide electrolytes at room temperature. c) Linear sweep voltammetry test using Mo foil as WE employing AA (in red), PA (in green), and BA (in blue) electrolytes. Measurements were obtained at a sweep rate of 0.1 mVs^{-1}. (For interpretation of the references to colour in this figure legend, the reader is referred to the Web version of this article.)

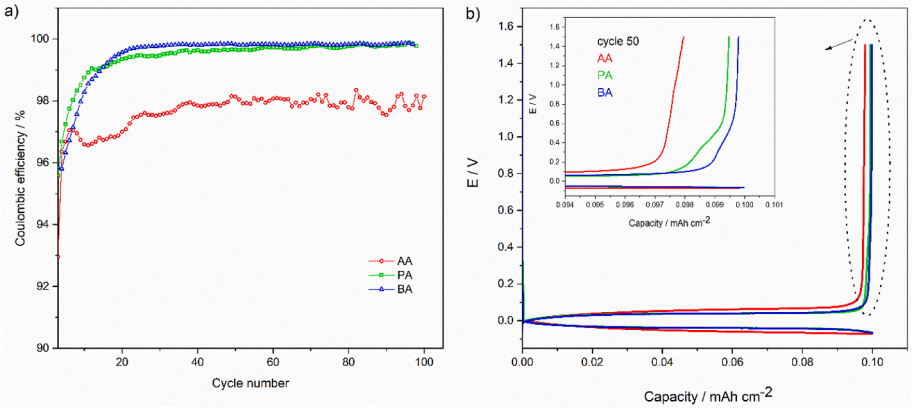

Fig. 2. a) Comparison of Coulombic efficiency of Al plating/stripping for AA, PA and BA electrolytes on Mo working electrode at 0.1 mA cm^{-2} for 1 h and b) corresponding voltage profile for 50th cycle of Al plating/stripping.

Table 1
Comparison of average Coulombic efficiency of amide-based electrolyte between conventional and macro-reversibility cycling.

Electrolyte	Conventional cycling efficiency (%)	Macro-reversibility efficiency (%)
AA	97.6	96.4
PA	98.9	99.4
BA	98.6	99.3

cyclic voltammetry, which confirmed reversible plating/stripping of amide-based electrolytes with pronounced activation in the initial cycles. Comparison with standard EA electrolyte revealed similar behavior, but lower current density for amide-based electrolytes (Fig. S4).

Al metal deposition was confirmed through energy dispersive spectroscopy (EDS) mapping of Al metal deposits. Mapping confirms the presence of Al metal in all three amide-based electrolytes, as well as in standard EA electrolyte (Fig. S5). Morphology investigations reveals more lamellar morphology of deposits in AA electrolyte, while other electrolytes display more compact morphology (Fig. S6). Observed difference in deposit morphology could contribute to worse adhesion of Al deposits and lowered Coulombic efficiency in AA electrolyte.

After evaluating amide-based electrolytes behavior at Al metal anode, we turned our attention towards electrolyte compatibility with organic cathode material, poly(anthraquinonyl sulfide) (PAQS), which would allow us to assess their applicability in full Al battery cell. PAQS polymer has already shown good electrochemical performance with reversible two electron reduction of conjugated carbonyl groups in both ionic liquid (EA) and urea $AlCl_3$-based electrolytes [11]. Moreover, due to the reversible redox potential of the anthraquinone group around 1.1 V vs. Al/Al^{3+}, it fits very well into the voltage stability window of amide-based electrolytes and serves as a suitable model compound. The cycling performance of the AA electrolyte at the C/4 rate exhibited an initial specific capacity of 121 mAh g^{-1}. PA exhibited a slightly higher initial capacity of 132 mAh g^{-1}, while BA exhibited the lowest initial capacity of 10.8 mAh g^{-1} due to high overpotential in the initial cycles (Fig. S7). Upon further cycling, the discharge capacity of the PAQS in BA electrolyte gradually increased and reached a maximum value of 114 mAh g^{-1} in the 20^{th} cycle (Fig. 3). The capacity drop is significant in the case of AA electrolyte, with less than 60 mAh g^{-1} obtained after 16 cycles. The capacity fade seems to be less pronounced in the PA electrolyte but there is clear evidence of side reactions close to the upper cut-off voltage limit of 1.8 V. This becomes more evident in later cycles and contributes to the lowered Coulombic efficiency of Al metal–organic cell (Fig. S7). The capacity fade seems to be the lowest in BA electrolyte, where more than 60 mAh g^{-1} of capacity is retained after 100 cycles.

Taking a look at the Coulombic efficiency, we observe interesting trends with initial efficiency above 100 % due to PAQS being in a charged state and incomplete active material utilization in the starting cycles. The highest efficiency is observed for AA electrolyte and is comparable with standard EA electrolyte in later cycles (Fig. S8). However, this is also connected to the relatively low reversible capacity in AA electrolyte. The efficiency of BA is lower, but still significantly better than one observed for PA electrolyte. These observations fit well with the anodic stability trends that were observed during LSV measurements with AA electrolyte displaying best oxidative stability. Although higher oxidative stability was expected from LSV, the decreased stability during cathode cycling is most likely caused by a significantly higher surface area of organic composite electrodes, which contain high surface area carbon additive. Decreased oxidative stability on high surface area carbon is confirmed through the cycling of electrodes composed of only carbon additive and PTFE binder, which confirms the presence of side reactions at the upper voltage limit of 1.8 V in both PA and BA electrolytes (Fig. S9). Cycling of carbon additive was also used to determine the real utilization rate of PAQS active material by removing the capacitive contribution of carbon black additive (Table S2) [30]. Real capacity utilization has shown that the maximum attainable capacities of PAQS active material are around 50 % of the theoretical capacity. Amide-based electrolytes display comparable utilization rates of active materials, which are slightly lower than in standard EA electrolyte.

To investigate the mechanism of the PAQS electrode in amide-based electrolytes, we conducted *ex situ* infrared (IR) analysis on organic electrodes harvested from pouch cells in the discharged and charged state. The characteristic IR peaks at 1671 cm^{-1} and 1651 cm^{-1} correspond to C=O vibrations (Fig. S10), and according to the two-electron reduction mechanism illustrated in Fig. 3c, we would expect these peaks to disappear if utilization is complete or to decrease in intensity in the case of partial utilization, which is the case here [31].

In all three amide-based electrolytes, the peaks at 1671 and 1651 cm^{-1} merge and lose intensity at the end of discharge, indicating a partial reduction of the organic electrode. The apparent reshaping of these peaks in the carbonyl region might also result from the presence of amide bands involved in complexation of Al species, as it is not noticeable in charged spectra [23]. Together with diminishing peaks corresponding to carbonyl stretching, a peak at around 1370 cm^{-1}, corresponding to C-O^- stretching, emerges, confirming the formation of the reduced state. A peak appearing at around 1400 cm^{-1} could result from C-N stretching band due to the presence of amides, which could indicate coordination of C-O^- groups with $AlCl_x^{(3-x)+}$ species.

Upon recharging, the peaks at 1671 and 1651 cm^{-1} of PAQS become distinguishable and regain their original intensity, while the enolate-related peak disappears. These changes are accompanied by a series of

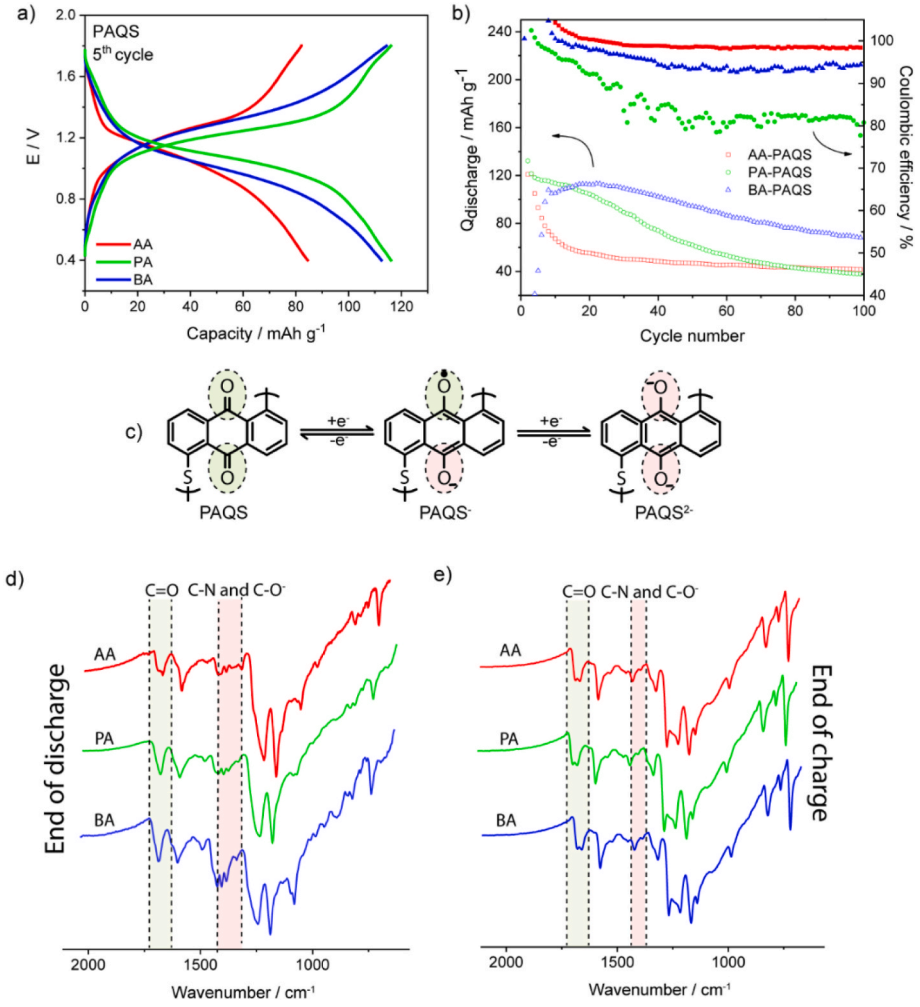

Fig. 3. a) 5th discharge/charge cycle at C/4 for PAQS electrodes in AA, PA and BA. b) Discharge capacity (left y-axis) and Coulombic efficiency (right y-axis) vs. cycle number of galvanostatic cycling test for 100 cycles at C/4. c) Electrochemical mechanism of PAQS active material. d) *Ex situ* PAQS electrodes in discharged and e) charged state.

peaks appearing and disappearing in the fingerprint region, consistent with previous observations [11]. This indicates a high degree of reversibility in the electrochemical reduction process. The consistency of these spectral changes across different electrolytes demonstrates that the fundamental mechanism of the organic electrode is preserved, whether EA or amide-based electrolytes are used.

However, one specific difference that we have observed, compared to our previous work using a standard EA electrolyte, is the absence of gradual degradation and additional sloping of the electrochemical plateau during long-term cycling of PAQS electrodes [11]. This was investigated in Al–PAQS cells with our Al electrolytes by plotting derivatives of galvanostatic curves (dQ/dE vs. E, Fig. S11). Derivative curves confirm the formation of additional reversible redox peak at lower potentials in EA electrolyte, while additional peak does not appear in any of the amide-based electrolytes, pointing to the peculiar behavior of EA electrolyte, most likely connected with EMIMCl IL and the potential utilization of large organic cation in the electrochemical mechanism.

4. Conclusion

A thorough investigation of three different $AlCl_3$ amide-based electrolytes with varying lengths of alkyl chain reveals that they can offer comparable electrochemical performance to standard EMIMCl-based electrolyte at a significantly lower price. Nevertheless, significant differences were observed between specific electrolytes and amides with longer alkyl chains (PA and BA) offer significantly better Al plating/stripping efficiency and lower overpotential than AA. From the point of oxidative stability, AA electrolyte enables slightly better oxidative stability, which is also confirmed in the testing of organic cathode material through the reduced Coulombic efficiency of PA and BA electrolyte and confirmed in testing of plain carbon additive-based electrodes. The capacity retention of organic cathode seems to be the best in the case of longer alkyl chains, with capacity fade being the fastest in AA, followed by PA and best retention in BA electrolyte. While capacity utilization is similar to EA electrolyte, the capacity retention is lower than in benchmark EA electrolyte. Although electrochemical mechanism of PAQS is equivalent to standard EA electrolyte, in all amide-based electrolytes, degradation of PAQS redox plateau as observed in EA electrolyte does not occur. This work opens up the possibilities for further exploration of longer chain amides such as valeramide and potential exploration of mixed amide electrolytes, which might lead to improvement of electrochemical performance and performance comparable to standard EA electrolyte. While Al plating/stripping metal efficiency in PA and BA is already very high, over 99 %, a pressing issue that remains to be addressed is the oxidative stability, which is limited to around 1.8 V and could severely decrease the choice of available cathode materials for Al batteries utilizing amide-based electrolytes.

CRediT authorship contribution statement

Matea Raić: Writing – review & editing, Writing – original draft, Investigation, Conceptualization. **Olivera Lužanin:** Writing – review & editing, Writing – original draft, Investigation. **Ivan Jerman:** Writing – review & editing, Writing – original draft, Investigation. **Robert Dominko:** Writing – review & editing, Conceptualization. **Jan Bitenc:** Writing – review & editing, Writing – original draft, Conceptualization.

Declaration of competing interest

The authors declare that they have no known competing financial interests or personal relationships that could have appeared to influence the work reported in this paper.

Data availability

Data will be made available on request.

Acknowledgement

M.R. would like to acknowledge the financial support of the Competitiveness and Cohesion Operational Programme, a project co-financed by the Croatian Government and the European.Union through the European Regional Development Fund (KK.01.1.1.01.0001). O. L., I. J., R. D. and J. B. would like to acknowledge the financial support of the Slovenian Research and Innovation Agency (ARIS) through research program P2-0423 and project J2-4462.

Appendix A. Supplementary data

Supplementary data to this article can be found online at https://doi.org/10.1016/j.jpowsour.2024.235575.

References

[1] European Commission, Study on the critical raw materials for the EU 2023 final report. https://doi.org/10.2873/725585, 2023.
[2] Y. Tian, G. Zeng, A. Rutt, T. Shi, H. Kim, J. Wang, J. Koettgen, Y. Sun, B. Ouyang, T. Chen, Z. Lun, Z. Rong, K. Persson, G. Ceder, Promises and challenges of next-generation "beyond Li-ion" batteries for electric vehicles and grid decarbonization, Chem. Rev. 121 (2021) 1623–1669, https://doi.org/10.1021/acs.chemrev.0c00767.
[3] W. Liu, Y. Li, H. Yang, B. Long, Y. Li, Y. Bai, C. Wu, F. Wu, Pursuing high voltage and long lifespan for low-cost Al-based rechargeable batteries: dual-ion design and prospects, Energy Storage Mater. 62 (2023) 102922, https://doi.org/10.1016/j.ensm.2023.102922.
[4] G.A. Elia, K.V. Kravchyk, M.V. Kovalenko, J. Chacón, A. Holland, R.G.A. Wills, An overview and prospective on Al and Al-ion battery technologies, J. Power Sources 481 (2021) 228870, https://doi.org/10.1016/j.jpowsour.2020.228870.
[5] J. Tu, W.L. Song, H. Lei, Z. Yu, L.L. Chen, M. Wang, S. Jiao, Nonaqueous rechargeable aluminum batteries: progresses, challenges, and perspectives, Chem. Rev. 121 (2021) 4903–4961, https://doi.org/10.1021/acs.chemrev.0c01257.
[6] Y. Zhang, S. Liu, Y. Ji, J. Ma, H. Yu, Emerging nonaqueous aluminum-ion batteries: challenges, status, and perspectives, Adv. Mater. 30 (2018) 1706310, https://doi.org/10.1002/adma.201706310.
[7] K.L. Ng, B. Amrithraj, G. Azimi, Nonaqueous rechargeable aluminum batteries, Joule 6 (2022) 134–170, https://doi.org/10.1016/j.joule.2021.12.003.
[8] M.C. Lin, M. Gong, B. Lu, Y. Wu, D.Y. Wang, M. Guan, M. Angell, C. Chen, J. Yang, B.J. Hwang, H. Dai, An ultrafast rechargeable aluminium-ion battery, Nature 520 (2015) 325–328, https://doi.org/10.1038/nature14340.
[9] P. Meng, Z. Yang, J. Zhang, M. Jiang, Y. Wang, X. Zhang, J. Luo, C. Fu, Electrolyte design for rechargeable aluminum-ion batteries: recent advances and challenges, Energy Storage Mater. 63 (2023) 102953, https://doi.org/10.1016/j.ensm.2023.102953.
[10] Z. Yang, F. Wang, P. Meng, J. Luo, C. Fu, Recent advances in developing organic positive electrode materials for rechargeable aluminum-ion batteries, Energy Storage Mater. 51 (2022) 63–79, https://doi.org/10.1016/j.ensm.2022.06.018.
[11] J. Bitenc, N. Lindahl, A. Vizintin, M.E. Abdelhamid, R. Dominko, P. Johansson, Concept and electrochemical mechanism of an Al metal anode – organic cathode battery, Energy Storage Mater. 24 (2020) 379–383, https://doi.org/10.1016/j.ensm.2019.07.033.
[12] J. Bitenc, U. Košir, A. Vizintin, N. Lindahl, A. Krajnc, K. Pirnat, I. Jerman, R. Dominko, Electrochemical mechanism of Al metal–organic battery based on phenanthrenequinone, Energy Mater. Adv. 2021 (2021) 9793209, https://doi.org/10.34133/2021/9793209.
[13] F.H. Hurley, T.P. Wier, The electrodeposition of aluminum from nonaqueous solutions at room temperature, J. Electrochem. Soc. 98 (1951) 207, https://doi.org/10.1149/1.2778133.
[14] B.S. Del Duca, Electrochemical behavior of the aluminum electrode in molten salt electrolytes, J. Electrochem. Soc. 118 (1971) 405, https://doi.org/10.1149/1.2408069.
[15] J. Robinson, R.A. Osteryoung, An electrochemical and spectroscopic study of some aromatic hydrocarbons in the room temperature molten salt system aluminum chloride-n-butylpyridinium chloride, J. Am. Chem. Soc. 101 (1979) 323–327, https://doi.org/10.1021/ja00496a008.
[16] H.M.A. Abood, A.P. Abbott, A.D. Ballantyne, K.S. Ryder, Do all ionic liquids need organic cations? Characterisation of [AlCl2·nAmide]+ AlCl4- and comparison with imidazolium based systems, Chem. Commun. 47 (2011) 3523–3525, https://doi.org/10.1039/c0cc04989a.
[17] A.P. Abbott, R.C. Harris, Y.T. Hsieh, K.S. Ryder, I.W. Sun, Aluminium electrodeposition under ambient conditions, Phys. Chem. Chem. Phys. 16 (2014) 14675–14681, https://doi.org/10.1039/c4cp01508h.
[18] E.L. Smith, A.P. Abbott, K.S. Ryder, Deep eutectic solvents (DESs) and their applications, Chem. Rev. 114 (2014) 11060–11082, https://doi.org/10.1021/cr300162p.
[19] D. Paterno, E. Rock, A. Forbes, R. Iqbal, N. Mohammad, S. Suarez, Aluminum ions speciation and transport in acidic deep eutectic AlCl 3 amide electrolytes, J. Mol. Liq. 319 (2020) 114118, https://doi.org/10.1016/j.molliq.2020.114118.
[20] M. Li, B. Gao, C. Liu, W. Chen, Z. Wang, Z. Shi, X. Hu, AlCl3/amide ionic liquids for electrodeposition of aluminum, J. Solid State Electrochem. 21 (2017) 469–476, https://doi.org/10.1007/s10008-016-3384-3.
[21] N. Canever, N. Bertrand, T. Nann, Acetamide: a low-cost alternative to alkyl imidazolium chlorides for aluminium-ion batteries, Chem. Commun. 54 (2018) 11725–11728, https://doi.org/10.1039/c8cc04468f.
[22] G.A. Elia, K. Hoeppner, R. Hahn, Comparison of chloroaluminate melts for aluminum graphite dual-ion battery application, Batter. Supercaps. 4 (2021) 368–373, https://doi.org/10.1002/batt.202000244.
[23] F. Jach, M. Wassner, M. Bamberg, E. Brendler, G. Frisch, U. Wunderwald, J. Friedrich, A low-cost Al-graphite battery with urea and acetamide-based electrolytes, Chemelectrochem 8 (2021) 1988–1992, https://doi.org/10.1002/celc.202100183.
[24] C. Liu, W. Chen, Z. Wu, B. Gao, X. Hu, Z. Shi, Z. Wang, Density, viscosity and electrical conductivity of AlCl3-amide ionic liquid analogues, J. Mol. Liq. 247 (2017) 57–63, https://doi.org/10.1016/j.molliq.2017.09.091.
[25] N. Lindahl, P. Johansson, Early stage techno-economic and environmental analysis of aluminium batteries, Energy Adv 2 (2023) 420–429, https://doi.org/10.1039/D2YA00253A.
[26] T. Pavčnik, M. Lozinšek, K. Pirnat, A. Vizintin, T. Mandai, D. Aurbach, R. Dominko, J. Bitenc, On the practical applications of the magnesium fluorinated alkoxyaluminate electrolyte in Mg battery cells, ACS Appl. Mater. Interfaces 14 (2022) 26766–26774, https://doi.org/10.1021/acsami.2c05141.
[27] I. Shterenberg, M. Salama, H.D. Yoo, Y. Gofer, J.-B. Park, Y.-K. Sun, D. Aurbach, Evaluation of (CF 3 SO 2) 2 N − (TFSI) based electrolyte solutions for Mg batteries, J. Electrochem. Soc. 162 (2015) A7118–A7128, https://doi.org/10.1149/2.0161513jes.
[28] Z. Song, H. Zhan, Y. Zhou, Anthraquinone based polymer as high performance cathode material for rechargeable lithium batteries, Chem. Commun. (2009) 448–450, https://doi.org/10.1039/B814515F.
[29] A.J. Lucio, I. Efimov, O.N. Efimov, C.J. Zaleski, S. Viles, B.B. Ignatiuk, A.P. Abbott, A.R. Hillman, K.S. Ryder, Amidine-based ionic liquid analogues with AlCl3: a credible new electrolyte for rechargeable Al batteries, Chem. Commun. 57 (2021) 9834–9837, https://doi.org/10.1039/d1cc02680a.
[30] J. Bitenc, K. Pirnat, O. Lužanin, R. Dominko, Organic cathodes, a path toward future sustainable batteries: mirage or realistic future? Chem. Mater. 36 (2024) 1025–1040, https://doi.org/10.1021/acs.chemmater.3c02408.
[31] A. Vizintin, J. Bitenc, A. Kopač Lautar, K. Pirnat, J. Grdadolnik, J. Stare, A. Randon-Vitanova, R. Dominko, Probing electrochemical reactions in organic cathode materials via in operando infrared spectroscopy, Nat. Commun. 9 (2018) 661, https://doi.org/10.1038/s41467-018-03114-1.